Discover Oncology

Research

Butyrate confers colorectal cancer cell resistance to anti-PD-1 therapy by promoting CPT1A-mediated fatty acid oxidation

Ran Zhu[1] · Shujiang Gu[2] · Yuan Tao[3] · Yan Zhang[4]

Received: 5 December 2024 / Accepted: 12 May 2025
Published online: 27 May 2025

Abstract
Immunotherapy including anti-PD-1 demonstrated therapeutic promise to colorectal cancer (CRC) patients, but tumor cell resistance limits their efficacy. Butyrate may influence therapeutic outcomes by modulating tumor metabolism, but it remains unclear whether butyrate influences CRC cell resistance to anti-PD-1 therapy. We aimed to investigate whether butyrate promotes resistance to anti-PD-1 therapy in CRC and underlying metabolic and immunologic mechanisms. CRC murine models were established by subcutaneously inoculating MC38 cells or butyrate/anti-PD-1-administered tumor cells of mice, followed by treatment with butyrate, anti-PD-1, or a combination. Therapeutic efficacy was assessed by tumor growth and survival outcomes. In vitro, HCT116 cells were exposed to monotherapy or co-therapy regimens. Carnitine Palmitoyltransferase 1A (CPT1A) knockdown was conducted by shRNA transfection both in vivo and in vitro. Fatty acid oxidation (FAO) was determined by oxygen consumption rate and CPT1A expression. CD8+ T cell cytotoxicity assays and CD8 expression in tumors were performed to evaluate immune cell infiltration. The addition of butyrate into anti-PD-1 treatment combination did not improve survival or reduce tumor volume compared to anti-PD-1 alone, with a marked activation of CPT1A observed in treated tumor tissues. Butyrate significantly elevated FAO, contributing to elevated oxygen consumption rate and reduced CD8+ T cell cytotoxicity. However, in sh-CPT1A models, the combination therapy significantly improved antitumor efficacy and restored CD8+ T cell infiltration. Furthermore, CRC patient samples resistant to anti-PD-1 therapy exhibited elevated CPT1A levels. Butyrate-induced CPT1A-mediated FAO promotes resistance to anti-PD-1 therapy in CRC, suggesting that targeting CPT1A might enhance the efficacy of immunotherapy.

Keywords Butyrate · CPT1A · Colorectal cancer · Fatty acid oxidation · Immune resistance · Anti-PD-1 therapy

1 Introduction

Colorectal cancer (CRC) is the third leading cause of cancer-related mortality worldwide, with a poor prognosis and high metastatic potential. Once metastasis occurs, fewer than 20% of patients survive beyond 5 years post-diagnosis [1]. Standard treatment options for CRC primarily involve systemic therapies, including cytotoxic chemotherapy,

Supplementary Information The online version contains supplementary material available at https://doi.org/10.1007/s12672-025-02686-x.

✉ Yan Zhang, zhangyan8023bobo@163.com; Ran Zhu, zhrky2011@163.com; Shujiang Gu, shujiang1981@sina.com; Yuan Tao, taotaowzx@163.com | [1]Department of Pathology, Changping Hospital of Integrated Chinese and Western Medicine, Beijing 102208, China. [2]Department of Laboratory Medicine, Beijing Changping Traditional Chinese Medicine Hospital, Beijing 102200, China. [3]Department of Gastroenterology, Beijing Changping Traditional Chinese Medicine Hospital, Beijing 102200, China. [4]Department of Pathology, Beijing Changping Traditional Chinese Medicine Hospital, South Section of Donghuan Road, Changping District, Beijing 102200, China.

biologic agents, immunotherapy, and their combinations [2]. Immunotherapy has emerged as a promising approach for improving patient outcomes and can be employed as either a first-line or subsequent treatment option [3].

Among immunotherapies, immune checkpoint inhibitors (ICIs) such as anti-PD-1 antibodies have shown significant efficacy in select CRC patients, resulting in extended overall survival in some cases [1, 4]. However, not all patients are able to benefit from this category of drugs due to various intrinsic and acquired resistance mechanisms, including genetic mutations, downregulation of immune targets such as PD-L1, and metabolic reprogramming [5, 6]. Since anti-tumor resistance pathways are key challenges that limit the effectiveness of anti-PD-1/PD-L1 ICIs, identifying and overcoming these resistance mechanisms is crucial for expanding the therapeutic benefits of immunotherapy to a broader population of CRC patients.

The gut microbiota and metabolites play a pivotal role in human health, with dysbiosis linked to the development and progression cancers including CRC [7, 8]. Among metabolites, butyrate has been associated with a reduced risk of CRC. Previous studies reported that butyrate exhibited antitumor properties by inhibiting histone deacetylase activity and associated signaling pathways, leading to oxidation and motility suppression in CRC cells [9, 10]. Additionally, butyrate contributes to a healthy intestinal environment by modulating inflammation and immune system, exerting preventive effect on CRC [11]. However, the role of butyrate in CRC progression may be more complex. Butyrate can enter cells and be metabolized in mitochondria via the fatty acid oxidation (FAO) pathway, enabling it to serve as a direct metabolic substrate for FAO and act as an alternative energy source [12]. Tumor cells adapt to the nutrient-scarce and hypoxic conditions of the tumor microenvironment (TME) by leveraging various metabolic pathways, especially the FAO pathway as it offers a higher energy yield than glucose oxidation [13, 14]. This increased energy support allows tumor cells to survive under metabolic stress and contributes to immunosuppressive conditions within the TME [15]. In addition, elevated FAO in tumor cells has been shown to impair T cell function, reduce immune cell infiltration, and weaken antitumor immunity [16]. Thus, while butyrate's role in CRC may have protective aspects, its metabolism through FAO may also facilitate mechanisms that support tumor survival and immune evasion.

The mechanism of anti-PD-1 therapy involves blocking receptors on activated T cells and improving the TME. Thus, butyrate-induced increases in FAO are likely to affect immune modulation and suppress T cell function within this context. However, this effect has yet to be completely clarified in CRC. In this study, we evaluated tumor growth, FAO, and its key rate-limiting enzyme Carnitine Palmitoyltransferase 1A (CPT1A) in CRC mouse models and cell lines treated individually or in combination with butyrate and anti-PD-1 therapy. To confirm the role of CPT1A in this process, we performed CPT1A knockdown to assess its impact on tumor metabolism and TME regulation. Additionally, to support the clinical relevance of these findings, we analyzed CPT1A expression in tumor samples from CRC patients treated with the anti-PD-1 antibody Nivolumab.

2 Material and methods

2.1 Ethics statement

All animal experiments were conducted in accordance with the guidelines for the Care and Use of Laboratory Animals as adopted by the National Institutes of Health and were approved by the Institutional Animal Care and Use Committee of Beijing Changping Traditional Chinese Medicine Hospital. Mice were housed in 22 ± 2 °C, 50 ± 10% humidity, 12-h light/dark cycle and were given ad libitum access to chow and water. All efforts were made to minimize suffering. Mice reached the ethical endpoints or at the end of the experiment were anesthetized by 2% maintenance concentration of isoflurane inhalation and humanely euthanized by cervical dislocation. The ethical endpoints were defined as tumor ulceration or when tumor volume exceeded 2000 mm^3.

For ethics of studies related to humans, all patient samples were collected under informed consent and in accordance with the ethical standards set forth by the Declaration of Helsinki. Ethical approval for this study was obtained from the Institutional Review Board of Beijing Changping Traditional Chinese Medicine Hospital. Tumor tissue samples were obtained from nine colorectal cancer patients undergoing anti-PD-1 immunotherapy with Nivolumab. Informed written consent was obtained from all participants prior to sample collection. Sample collection and analysis were conducted at Beijing Changping Traditional Chinese Medicine Hospital and Department of Pathology, Changping Hospital of Integrated Chinese and Western Medicine following protocols designed to protect patient confidentiality and maintain sample integrity.

2.2 Patient classification criteria

After anti-PD-1 immunotherapy, 9 CRC patients were stratified into PD-1 sensitive group (PD-1 S, n = 5) and PD-1 resistant group (PD-1 R, n = 4) based on their response to therapy. Classification criteria followed imaging assessments, biomarker levels and clinical response assessments, with PD-1 S patients exhibiting either partial response or stable disease and PD-1 R patients demonstrating progressive disease, new metastatic lesions, or other indicators of disease advancement per RECIST criteria [17, 18]. Tumor tissues were snap-frozen in liquid nitrogen and stored at −80 °C until analysis of the expression of CPTA1 level.

2.3 Animal experiment schedule

Female C57BL/6 mice (6–8 weeks old, 15–17 g) were used to establish CRC tumor models via subcutaneous injection of 1×10^6 MC38 cells (ATCC, Manassas, VA, USA) [19]. Tumors were allowed to grow for 8–10 days until they reached 50–70 mm^3 in volume, at which point mice were randomized into treatment groups (n = 6 per group): Control, α-PD-1, butyrate, and butyrate/α-PD-1. Mice in the α-PD-1 group received anti-PD-1 (200 μg/mouse, Bio X Cell, West Lebanon, NH, USA) intraperitoneally, while the butyrate group received sodium butyrate (0.25 μmol/mouse, Sigma-Aldrich, St. Louis, MO, USA) via intratumoral injection. The Butyrate/α-PD-1 group received both treatments as described. Control mice received saline (0.9% NaCl) and 200 μg IgG. Treatments were administered twice weekly for 28 days.

To investigate the effects of butyrate supplementation on α-PD-1 therapy, the treatment period was extended to 60 days or until ethical endpoints for a separate cohort, allowing for survival monitoring. For mechanistic insights into butyrate's role in inducing anti-PD-1 resistance and regulating FAO enzyme expression, tumor cells were isolated from butyrate/α-PD-1-treated mice (butyrate/α-PD1 MC38 cells) and injected into a new cohort of mice, then compared with mice inoculated with standard MC38 cells, with either IgG or α-PD-1 administration. To assess the specific involvement of CPT1A in butyrate-induced resistance, additional CRC models were generated using MC38 cells transfected with either control shRNA (sh-NC) or CPT1A-targeted shRNA (sh-CPT1A). These models were treated either individually or with combination regimen (n = 5).

At the end of treatments, mice were euthanized for tumor tissue separation followed by therapeutic efficacy and mechanism-related evaluation. The IACUC protocol in this study follows the guidelines for the ethical review of laboratory animal welfare People's Republic of China National Standard GB/T 35892–2018 [20]. The maximal tumor size/burden was not exceeded the permissible tolerance in IACUC protocol (< 2 cm).

2.4 Therapy effect evaluation

Tumor imaging and weight measurement were conducted to evaluate the therapeutic efficacy in each treatment group. Tumor images were captured using a high-resolution digital camera (Nikon D7500, Nikon Corporation, Tokyo, Japan) and then weighted by an analytical balance. Tumor volume was measured every 3 or 5 days using digital calipers and volumes were calculated as: $(\text{length} \times \text{width}^2) \times 0.5$. Survival data were recorded to construct survival curves.

2.5 Cell maintenance and treatment

HCT116 cells were obtained from the ATCC and cultured in Dulbecco's Modified Eagle Medium (DMEM; Gibco, Waltham, MA, USA) supplemented with 10% fetal bovine serum (FBS) and 1% penicillin–streptomycin [19]. HCT116 cells were exposed to 5 mM sodium butyrate or left untreated for 6 h.

For co-culture experiments, HCT116 cells with or without CPT1A silencing were added with CD8+ T cells (TALL-104 cell line, ATCC) at an effector-to-target ratio of 10:1. Treatment groups were set up as follows: control, butyrate (5 mM), α-PD1 (10 μg/mL), and butyrate combined with α-PD1. Additional wells containing only target cells (HCT116) or only effector cells (TALL-104) were included as control. Co-cultures were incubated for 24 h in a humidified incubator at 37 °C with 5% CO_2 for further assays.

2.6 Cell transfection

HCT116 cells were transfected with shRNA constructs targeting CPT1A to achieve gene knockdown. Cells were cultured overnight to reach 60–70% confluence. For transfection, shRNA plasmids specific to CPT1A (sh1-CPT1A and sh2-CPT1A) or a non-targeting control shRNA (sh-NC) were obtained from Genechem (Shanghai, China). Transfection was performed using Lipofectamine 3000 reagent (ThermoFisher Scientific, Waltham, MA, USA) according to the manufacturer's protocol. Briefly, 2 μg of plasmid DNA and 6 μL of Lipofectamine 3000 were diluted separately in Opti-MEM medium (Gibco) and incubated for 10 min before adding to cells. Subsequently, transfected cells were incubated for 48 h under standard culture conditions, after which knockdown efficiency was confirmed by quantitative PCR (qPCR) and Western blot analysis. Cells with higher transfection efficiency were used in downstream functional assays.

2.7 Oxygen consumption rate (OCR) measurement

The OCR of HCT116 cells was measured using the Seahorse XF24 Extracellular Flux Analyzer (Agilent Technologies, Santa Clara, CA, USA) following manufacturer protocols. After 6-h incubation of butyrate-treated HCT116 cells or 48-h incubation for sh-CPT1A and their controls, cells were washed and incubated in Seahorse XF base medium supplemented with 10 mM glucose, 2 mM L-glutamine, and 1 mM pyruvate (pH 7.4) for 1 h at 37 °C in a CO_2-free environment. The OCR measurements were taken at baseline and following the equential injection of 1 μM oligomycin, 1 μM FCCP, and a mixture of rotenone and antimycin A (0.5 μM each). Data were analyzed using Wave software (Agilent Technologies).

2.8 Cytotoxicity assay

The Cell Counting Kit-8 (CCK-8; Dojindo Laboratories, Kumamoto, Japan) was used to evaluate cytotoxicity. After 24 h of co-culture with treatment, 10 μL of CCK-8 solution was added to each well, followed by a further 2-h incubation at 37 °C in a 5% CO_2 atmosphere. Absorbance was measured at 450 nm using a microplate reader (SpectraMax iD3, Molecular Devices, San Jose, CA, USA). Cytotoxicity was calculated as: $\text{Cytotoxicity}\ (\%) = \left(1 - \frac{A_{test\ well} - A_{effector\ well}}{A_{target\ well}}\right) \times 100\%$. $A_{\text{test well}}$ and $A_{\text{target well}}$ represents the absorbance of wells containing both target and effector cells. $A_{\text{effector well}}$ is the absorbance with only effector cells and target cells, respectively.

2.9 qPCR

qPCR was employed to assess the transfection efficiency of two types of sh-RNAs in HCT116 cells or mRNA expression of clinical samples. Total RNA was extracted from the transfected cells post-transfection or collected tumor tissues using the RNeasy Mini Kit (Qiagen, Hilden, Germany) according to the manufacturer's instructions. The concentration and purity of the RNA were measured using a NanoDrop 2000 spectrophotometer (ThermoFisher Scientific). RNA was reverse transcribed into cDNA using the PrimeScript RT Reagent Kit (Takara Bio, Shiga, Japan). qPCR was performed using the SYBR Green Master Mix (Applied Biosystems, ThermoFisher Scientific) on a CFX96 Touch Real-Time PCR Detection System (Bio-Rad, CA, USA). A total of 20 μL PCR reaction mixture included SYBR Green Master Mix, CPT1A-specific primers (Supplementary Table 1), cDNA template and nuclease-free water for 10 μL, 0.4 μL, 2 μL, and 7.2 μL, respectively. The relative expression levels of the target genes were calculated using the $2^{-\Delta\Delta Ct}$ method and normalized to β-Actin expression.

2.10 Western blot analysis

Transfected cells or collected animal or clinical tumor tissues were washed with cold PBS before being homogenized in RIPA lysis buffer (ThermoFisher Scientific) containing protease and phosphatase inhibitors (Roche, Basel, Switzerland). Tumor homogenates were incubated on ice for 30 min with periodic vortexing. Cell and tissue lysates were then centrifuged and the concentration of extracted proteins was determined using the BCA Protein Assay Kit (ThermoFisher Scientific), in accordance with the manufacturer's protocol. Equal amounts of protein were then separated by SDS-PAGE, which were subsequently transferred to a PVDF membrane (Bio-Rad) using a Trans-Blot Turbo Transfer System (Bio-Rad). Afterwards, the membranes were blocked with 5% skim milk and incubated overnight at 4 °C with 1: 500 diluted primary antibodies against CPT1A and/or CPT1B, as detailed in Supplementary Table 2. The membranes were subsequently incubated with HRP-conjugated secondary IgG antibody (1: 2000; Abcam, Cambridge, UK) for 1 h and washed before

protein bands were visualized using SuperSignal West Pico PLUS Chemiluminescent Substrate (ThermoFisher Scientific) on a ChemiDoc XRS + Imaging System (Bio-Rad). β-Actin was used for normalization. Western blot bands were analyzed with Image Lab Software (Bio-Rad).

2.11 Immunohistochemistry (IHC)

IHC was performed to assess CPT1Aexpression in CRC tumor tissues. Excised tumor tissues were fixed in 10% neutral-buffered formalin for 24 h, then embedded in paraffin and sectioned. Paraffin sections were deparaffinized in xylene and rehydrated before being heated in citrate buffer (Abcam). After cooling to room temperature, slides were incubated with 3% hydrogen peroxide for 10 min. Blocking was performed using 5% bovine serum albumin prior to antibody incubation. Sections were incubated overnight at 4 °C with a primary antibody against CPT1A (1:200; Supplementary Table 2). Following three washes in PBS, sections were incubated with a biotinylated secondary antibody (1:500; Abcam) for 1 h. Signal detection was achieved using a VECTASTAIN® ABC Kit (Vector Laboratories, Burlingame, CA, USA) and diaminobenzidine substrate (ThermoFisher Scientific), with hematoxylin used for counterstaining. Slides were then dehydrated, cleared, and mounted with coverslips. Images were captured using a digital microscope (Olympus BX53, Olympus Corporation, Tokyo, Japan) at 20 × magnification.

2.12 Immunofluorescence staining

Paraffin-embedded tumor tissue sections were deparaffinized and rehydrated. Antigen retrieval was performed using citrate buffer (pH 6.0) at 95 °C for 15 min. After blocking with 5% bovine serum albumin for 1 h, sections were incubated overnight at 4 °C with anti-CD8 antibody (1:200; ThermoFisher Scientific). After washing, sections were incubated with FITC-conjugated secondary antibody (1:500; ThermoFisher Scientific) for 1 h at room temperature. Nuclei were counterstained with DAPI. Fluorescent images were captured using the Olympus BX53 microscope.

2.13 Statistical analysis

Data were tested for normality using the Shapiro–Wilk test. Statistical significance was assessed by one-way analysis of variance or the Kruskal–Wallis test with Bonferroni's post hoc test for comparisons among multiple groups using Prism software (Graphpad Software, Inc., CA, USA). Data are expressed as standard error of the mean ± standard deviation (SEM ± SD) and $p < 0.05$ was considered statistically significant.

3 Results

3.1 Butyrate/anti-PD1 combination demonstrates no enhanced antitumor efficacy in colorectal cancer mice

Following the successful establishment of colorectal cancer in murine models, drug treatments were administered, with tumor size monitored every 5 days. Tumor volume was measured to evaluate treatment efficacy, and a threshold of 2000 mm^3 or severe ulceration prompted ethical euthanasia. The study was concluded at 60 days if mice survived without reaching these criteria. As shown in Fig. 1A, tumor growth curves indicated a persistent increase in tumor volume across all groups. Tumor growth was most rapid in the control, with drug-treated groups showing a degree of growth inhibition compared to controls. Notably, despite the butyrate/α-PD1 combination group exhibited a slightly slower tumor growth rate than the other groups during the first 20 days, tumor growth accelerated subsequently and no significant enhancement in inhibition compared to mice administrated with monotherapies alone. In terms of survival (Fig. 1B), only the butyrate-treated group demonstrated extended survival, with 33% (2 of 6) of mice remaining alive by the end of the study. In contrast, all mice in the control group succumbed by day 42. In addition, even if mice in the α-PD1 and butyrate/α-PD1 combination groups experienced later mortality compared to the control, no survival benefit was observed from combination treatment compared to the α-PD1 group. The addition of butyrate to α-PD1 may even reduce the therapeutic efficacy of α-PD1, as mice treated with butyrate + α-PD1 showed mortality 4 days earlier. These indicated that butyrate/α-PD1 combination did not enhance the antitumor effect of anti-PD1 therapy and probably contributed to anti-PD1 treatment resistance.

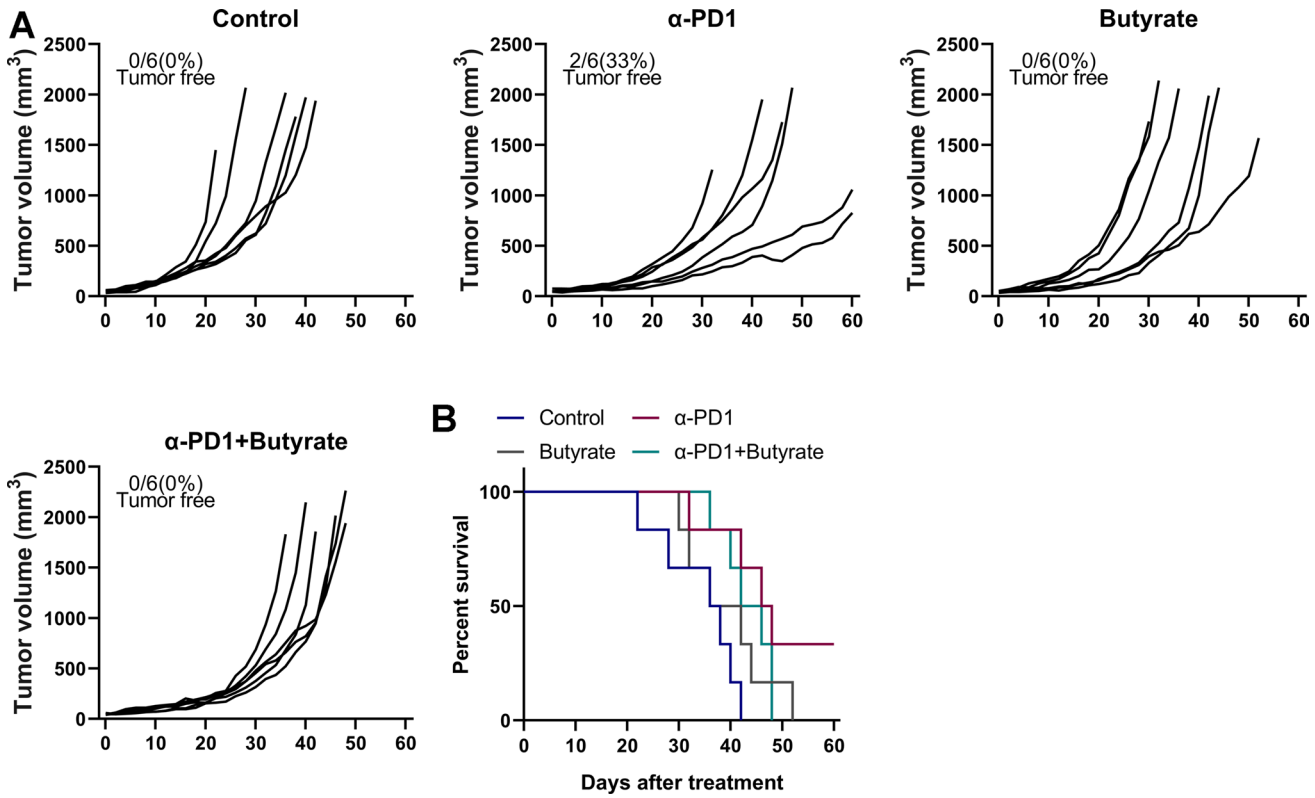

Fig. 1 Butyrate/α-PD1 combination did not improve antitumor efficacy in colorectal cancer murine models. After successful subcutaneous inoculation with MC38 cells to establish the colorectal cancer model, mice were administered butyrate, α-PD1 alone, or in combination, with saline and IgG injections used as the control. **A** Tumor volumes were measured every 5 days. Tumor size threshold for ethical euthanasia was set at 2000 mm^3 or upon detection of severe ulceration. **B** Survival curves were generated until the ethical end or 60 days from treatment

3.2 Butyrate/anti-PD1 combination induces anti-PD-1 therapy resistance and CPT1A activation in tumor tissues

To investigate whether butyrate contributes to resistance against anti-PD-1 therapy, tumor cells were isolated from mice treated with the butyrate/α-PD1 combination (butyrate/α-PD1 MC38 cells) for further assays. These cells were then subcutaneously inoculated into naive mice, with other mice receiving original MC38 cells. Once tumor volumes reached 50–70 mm^3, mice were received either IgG as a control or α-PD1 therapy for 28 days, after which tumors were collected for evaluation (Fig. 2A). As observed in the tumor images, α-PD1 treatment significantly inhibited tumor growth in mice inoculated with MC38 cells, whereas tumors in the butyrate/α-PD1 MC38 cell-inoculated mice showed limited response to α-PD1 treatment, appearing mostly comparable to the IgG control group (Fig. 2B). Consistent with visual observations, both tumor volume and tumor weight measurements confirmed this pattern after 28 days of treatment. Tumors in the MC38 + IgG group were significantly larger in size and weight compared to those in the MC38 + α-PD1 group, while no statistical difference was noted between the butyrate/α-PD1 MC38 + IgG and butyrate/α-PD1 MC38 + α-PD1 groups (Fig. 2C, D). To further understand the underlying mechanisms, key enzymes involved in FAO were examined. Western blot (WB) analysis revealed that baseline levels of CPT1A and CPT1B were elevated in tumor tissues from butyrate/α-PD1 MC38 cell-inoculated mice with IgG administration compared to those in MC38 cell-inoculated counterparts. Post-treatment with α-PD1, CPT1A expression was further elevated in the butyrate/α-PD1 MC38 + α-PD1 group relative to its IgG control. However, no difference of CPT1B expression was found in these two groups, although it was upregulated in the MC38 + α-PD1 group as compared to its IgG counterpart (Fig. 2E). Additionally, IHC demonstrated a marked increase in CPT1A expression in tumor tissues derived from butyrate/α-PD1 MC38 cell-inoculated mice (Fig. 2F). These collectively suggested that the butyrate/α-PD1 combination may induce resistance to anti-PD-1 therapy, potentially through the upregulation of CPT1A.

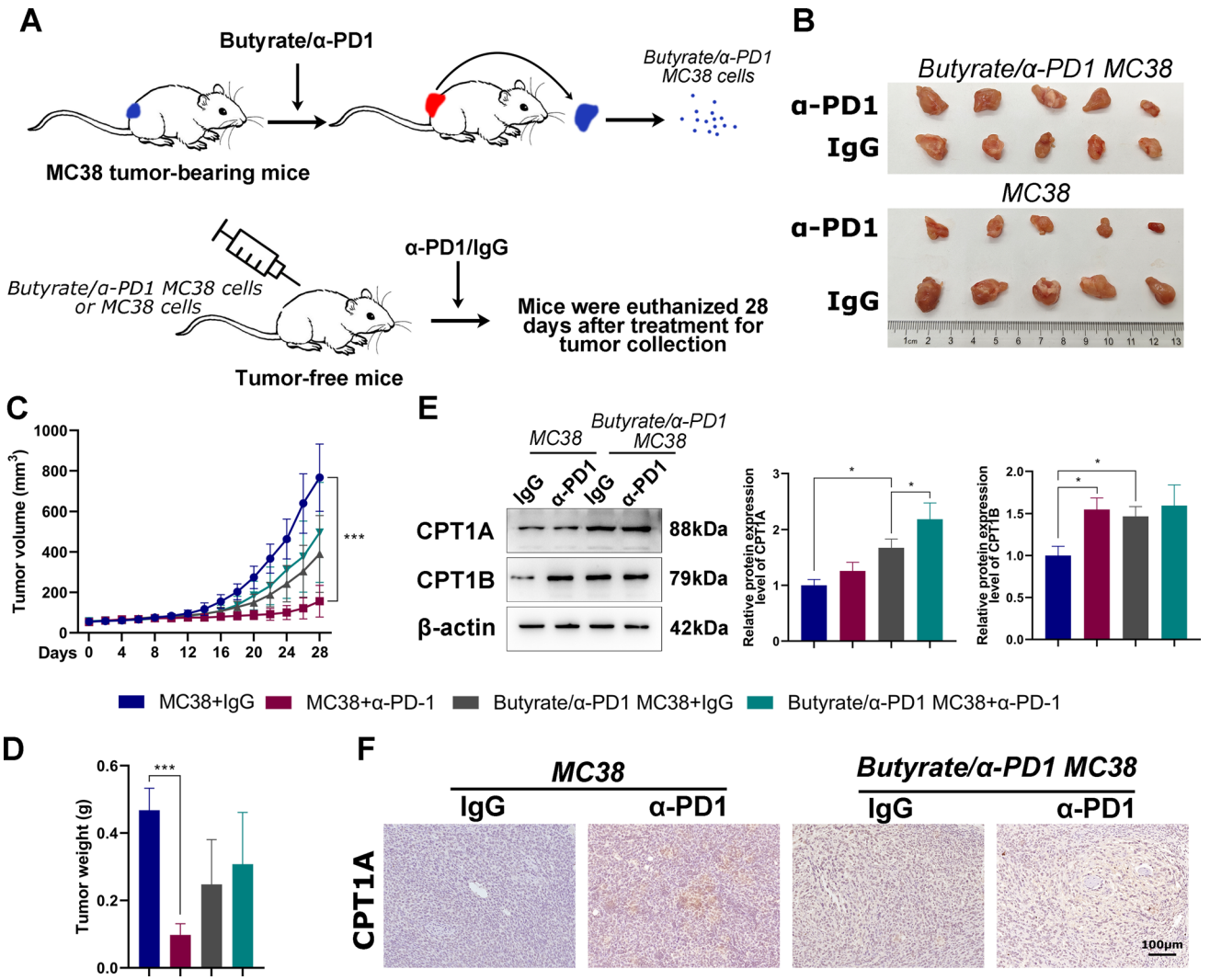

Fig. 2 Butyrate/α-PD1 combination induces anti-PD-1 therapy resistance and CPT1A activation in colorectal tumor tissues. **A** Schematic of experimental design. Tumor cells isolated from mice treated with Butyrate/α-PD1 combination therapy (Butyrate/α-PD1 MC38 cells) were inoculated subcutaneously into naive mice, with original MC38 cells injected as a control. After the transplanted tumor model was established, mice treated with IgG or α-PD1 for 28 days, at which **B** tumor images, **C** tumor volumes and **D** weight were assessed. **E** Western blot analysis was conducted to determine CPT1A and CPT1B protein expression. **F** Immunohistochemistry analysis was used for CPT1A expression evaluation in tumor tissues, with images captured at a magnification of 200×. Data are presented as mean ± SEM. *$p < 0.05$, ***$p < 0.001$

3.3 Butyrate enhances CPT1A-mediated fatty acid oxidation and reduces α-PD1-induced cytotoxicity in HCT116 cells

To explore the mechanistic role of CPT1A-mediated FAO in butyrate's modulation of antitumor efficacy, the OCR of HCT116 cells treated with 5 mM butyrate for 6 h was initially assessed. As shown in Fig. 3A, OCR was significantly elevated in the butyrate-treated group compared to untreated cells during the 63–81 min phase, suggesting the increased FAO level induced by butyrate. This increase in metabolic activity correlated with elevated protein expression levels of both CPT1A and CPT1B, as indicated by Western blot analysis (Fig. 3B), further supporting butyrate's role in promoting FAO. Subsequently, co-culture experiments were conducted with HCT116 cells and CD8+ T cells with diverse treatment. After a 24-h treatment, followed by a 2-h exposure to CCK-8, both α-PD1 and butyrate treated cells demonstrated increased cytotoxicity relative to the control. However, the combined butyrate/α-PD1 treatment resulted in a significantly reduced cytotoxicity compared to α-PD1 alone, achieving levels comparable to butyrate monotherapy (Fig. 3C). To further verify the involvement of CPT1A in these observations, CPT1A knockdown was performed using two shRNA constructs,

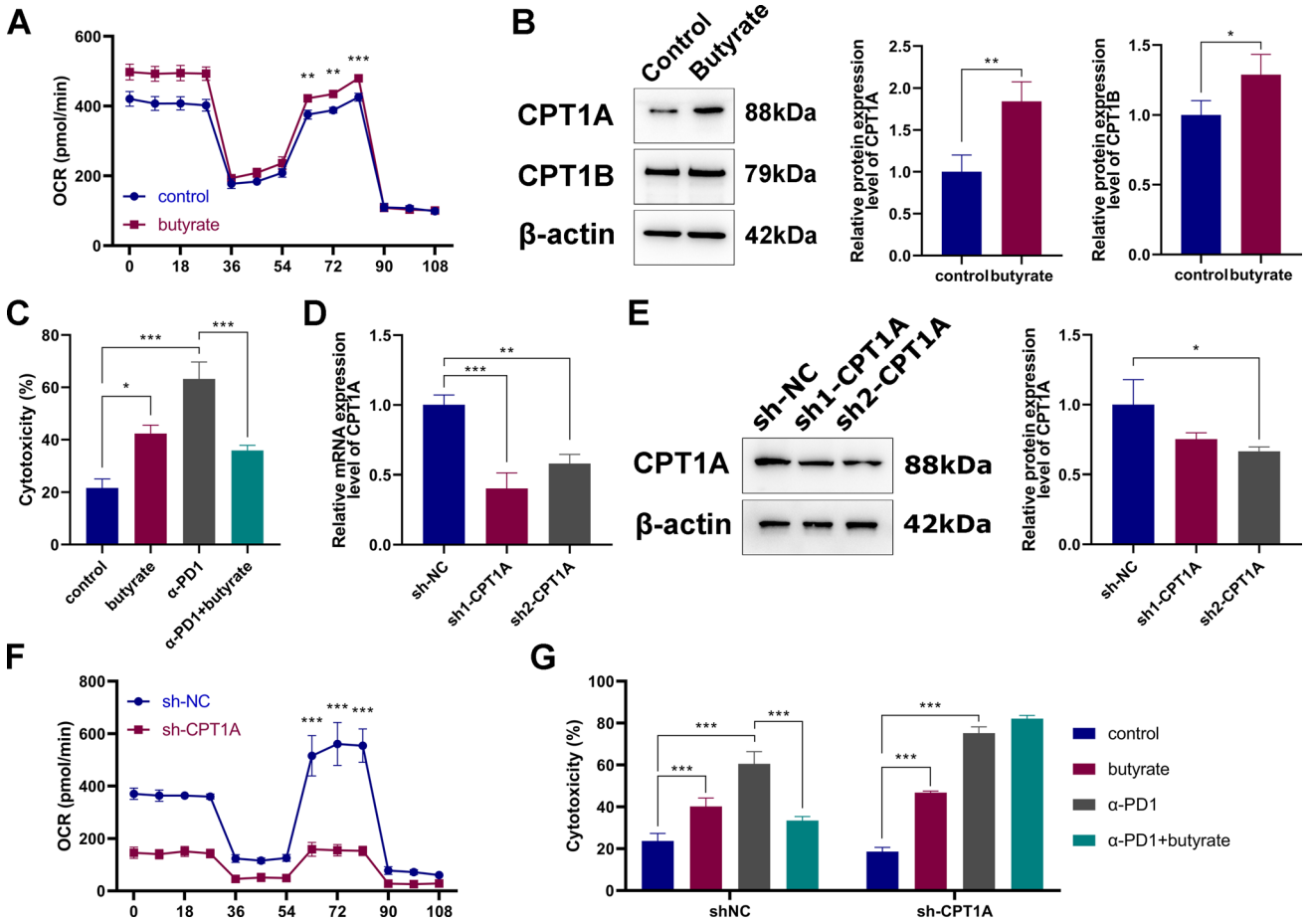

Fig. 3 Butyrate enhances CPT1A-mediated fatty acid oxidation (FAO) and reduces α-PD1-induced cytotoxicity in vitro. HCT116 cells were treated with 5 mM butyrate for 6 h. After that, **A** Oxygen consumption rate (OCR), **B** CPT1A and CPT1B protein expression were determined by Seahorse XF24 extracellular flux analyzer and Western blot analysis, respectively. CD8+ T cells were co-cultured with HCT116 cells at a ratio of 10:1. Following 24-h treatment with α-PD1, butyrate, or their combination, **C** cytotoxicity was assessed via 2-h CCK-8 exposure. Subsequently, sh-NC and two types of sh-CPT1A were transfected to HCT116 cells. **D** CPT1A mRNA and **E** protein levels were determined by quantitative PCR and Western blotting, respectively, to evaluate transfection efficiency. sh2-CPT1A with a higher transfection efficiency was selected for further assays. **F** OCR assessment in CPT1A knockdown cells and (**G**) cytotoxicity assay in those co-cultured with CD8+ T cells prior to being treated with distinct therapies were conducted to evaluate FAO activation and capability of immune cells. Data are presented as mean ± SEM. *p < 0.05, **p < 0.01, ***p < 0.001

sh1-CPT1A and sh2-CPT1A. qPCR showed that both shRNA constructs effectively suppressed CPT1A mRNA expression (Fig. 3D), but only sh2-CPT1A significantly reduced CPT1A protein levels compared to the sh-NC control (Fig. 3E), leading to its selection for subsequent experiments. Following CPT1A knockdown and butyrate treatment, OCR was notably lower in the sh2-CPT1A group than in the sh-NC control during the 63–81 min period (Fig. 3F), confirming CPT1A's role in butyrate-enhanced oxidative metabolism. In co-culture assays with CD8+ T cells, the decreased cytotoxicity observed with butyrate/α-PD1 combination treatment in sh-NC cells was reversed in sh2-CPT1A cells, showing no significant difference from α-PD1 monotherapy (Fig. 3G). This suggests that CPT1A-mediated FAO induced by butyrate may contribute to the observed reduction in α-PD1-induced cytotoxicity, highlighting a potential mechanism by which butyrate modulates immune response and contributes to therapeutic resistance in HCT116 cells.

3.4 CPT1A upregulation correlates with resistance to anti-PD-1 therapy in colorectal cancer patients

To further elucidate the involvement of CPT1A in mediating resistance to anti-PD-1 therapy in clinical context, CPT1A expression levels were examined in tumor tissues from nine CRC patients treated with the Nivolumab. We collected 5 PD-1 S patients and 4 PD-1 R patients based on the development of immune resistance post-treatment. qPCR analysis revealed a significantly higher expression of CPT1A mRNA in the PD-1 R group compared to the PD-1 S group (Fig. 4A).

This was further supported by IHC and Western blot analysis, which demonstrated increased CPT1A protein expression in the PD-1 resistance patients relative to the sensitive counterparts (Fig. 4B, C). Elevated CPT1A levels in the PD-1 R patient across multiple detection methods indicated that CPT1A could be contributing to an adaptive resistance mechanism.

3.5 CPT1A deficiency improves the antitumor efficacy of butyrate/anti-PD1 combination therapy in mice

To evaluate the role of CPT1A in modulating the antitumor response to butyrate/anti-PD1 combination therapy in vivo, MC38 cells were subcutaneously injected into mice with either sh-NC or sh-CPT1A modifications. Mice were received injections of IgG, α-PD1, butyrate, or butyrate/α-PD1 for 28 days when tumor volumes reached 50–70 mm^3. Tumor volume was recorded every three days to assess treatment efficacy. In sh-NC mice, tumor volumes in the butyrate/α-PD1 combination group were larger than in the α-PD1 monotherapy group, suggesting no additional benefit from the combination therapy. However, in sh-CPT1A mice, the butyrate/α-PD1 combination exhibited a stronger inhibitory effect on tumor volume growth compared to α-PD1 alone, with tumors also significantly smaller than in the IgG control group (Fig. 5A). Representative tumor images corroborated these findings, showing minimal size reduction with butyrate/α-PD1 treatment in the sh-NC group compared to controls, while in the sh-CPT1A group, the combination therapy yielded visibly smaller tumors than in both the IgG control and two monotherapy groups (Fig. 5B). Tumor weight followed a similar trend. While the butyrate/α-PD1 treatment did not significantly reduce tumor weight in the sh-NC group and even counteracted the weight reduction observed with α-PD1 alone, it substantially reduced tumor weight when CPT1A was knockdown, even lower than with α-PD1 monotherapy (Fig. 5C). Immunofluorescence staining for CD8 expression within tumor tissues revealed no significant difference between IgG and butyrate/α-PD1 groups in sh-NC mice. However, in sh-CPT1A treated models, CD8 expression was markedly higher in the butyrate/α-PD1 group than the α-PD1 monotherapy counterparts, suggesting enhanced T-cell infiltration (Fig. 5D). These results collectively illustrated that the absence of CPT1A reversed the resistance to immune checkpoint inhibitors induced by butyrate and strengthened the antitumor efficacy of butyrate/α-PD1 therapy, likely via enhancing immune cell infiltration.

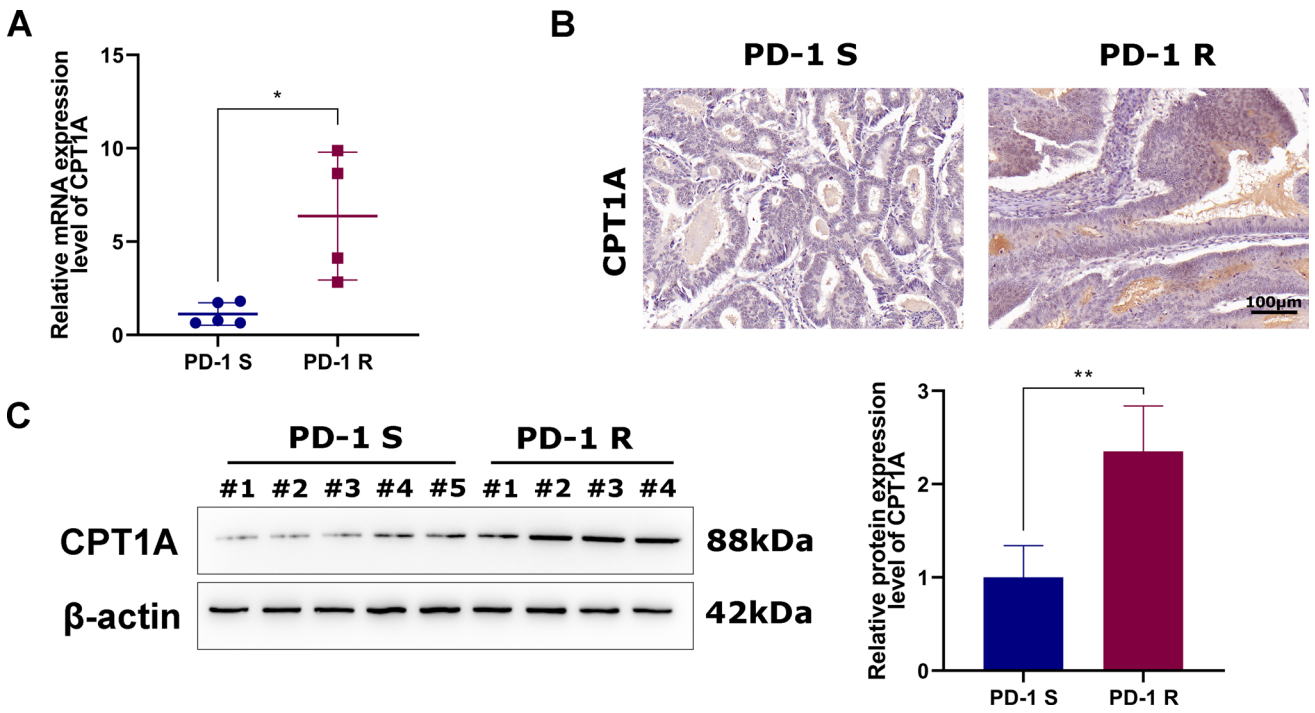

Fig. 4 CPT1A upregulation correlates with resistance to anti-PD-1 therapy in colorectal cancer (CRC) patients. Tumor tissues from CRC patients treated with Nivolumab were collected to assess **A** CPT1A mRNA levels, and **B**, **C** protein expression via quantitative PC, immunohistochemistry and Western blot analysis, respectively. Data are presented as mean ± SEM. *$p < 0.05$, **$p < 0.01$. PD-1 S: PD-1 sensitive, n = 5; PD-1 R: PD-1 resistant, n = 4

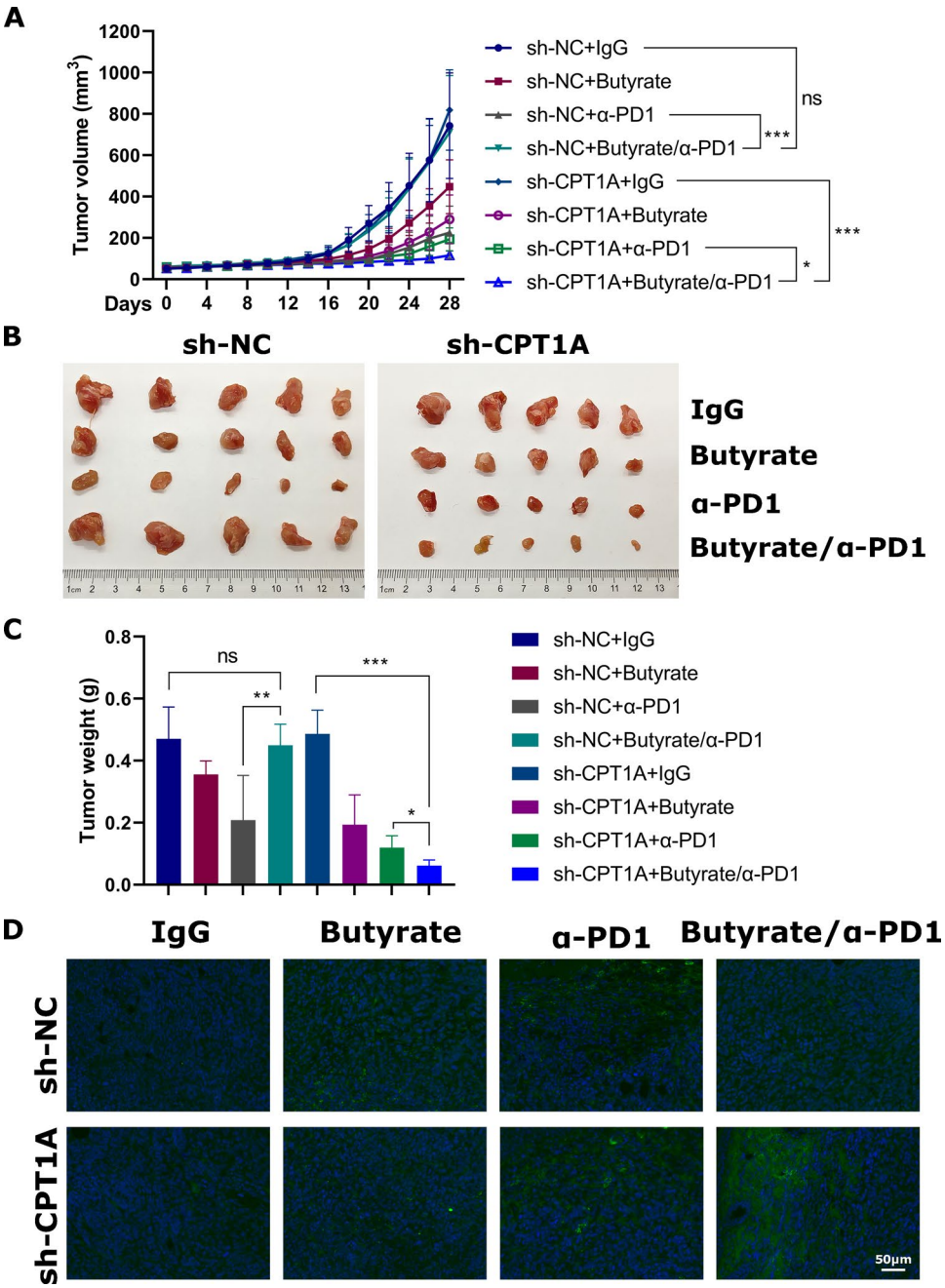

Fig. 5 CPT1A deficiency improves the antitumor efficacy of butyrate/α-PD1 combination therapy in colorectal cancer mice. Mice were subcutaneously inoculated with sh-NC or sh-CPT1A-tranfected MC38 cells to establish the colorectal cancer model. Butyrate, α-PD1, or butyrate/α-PD1 combination were used for 28-day therapy. **A** Tumor volume progression was measured every three days. After treatment, tumors were collected to take **B** representative images and determine **C** tumor weight. **D** Immunofluorescence staining was performed to evaluate CD8+ T cell infiltration, CD8 + cells are stained in red, and nuclei are counterstained with DAPI (blue). Data are presented as mean ± SEM. *p < 0.05, **p < 0.01, ***p < 0.001. *ns* no significance

4 Discussion

CRC accounts for approximately 10% of all cancer cases and related mortality, imposing a substantial social and economic burden worldwide [21]. While immunotherapy has emerged as a promising treatment to offer significant benefits to CRC patients, therapeutic resistance remains a primary challenge that limits its effectiveness [22]. As such, understanding the mechanisms underlying resistance to ICIs is crucial to improving clinical outcomes. In our present study, we demonstrated that butyrate, a gut flora metabolite can induce resistance to anti-PD-1 therapy in CRC by enhancing CPT1A-mediated FAO. Through a series of in vitro and in vivo experiments, we established that butyrate upregulates CPT1A, which not only promoted FAO to drive metabolic reprogramming but also diminished CD8 + T cell effect, including cytotoxic responses against HCT116 and immune infiltration within tumor tissues.

The impact of butyrate on cancer remains unclear, often described as the "butyrate paradox" [23, 24]. Our findings provide laboratory evidence supporting a restrictive effect of butyrate on CRC under certain conditions. In the context of the combination of it with other anti-tumor drugs, a recent report indicated that butyrate can significantly enhance the efficacy of anti-PD-1 therapy in mice bearing CT26 tumors, which is in contrast of our findings [25]. In our present results, while butyrate monotherapy offered a survival advantage in CRC mouse models, adding butyrate to α-PD-1 did not improve survival outcomes. Additionally, butyrate/α-PD-1 MC38 cell-inoculated CRC mice showed reduced sensitivity to α-PD-1, which was comparable to the IgG control. This suggests the existence of a "butyrate paradox" also in combination therapies. One potential reason for the contrasting therapeutic outcomes could be the dosing regimen, in which the former study administered a daily dose of 150 mM, whereas our study employed a significantly lower dose of only 0.25 μmol, administered twice weekly. The impact of dosage on the synergistic or antagonistic effects of butyrate might require further investigation.

To further understand the mechanisms underlying the resistance brought by butyrate in combination with anti-PD-1 therapy, we conducted in-depth investigations. We identified significant CPT1A activation in butyrate/α-PD1 MC38 + α-PD-1 treated mice. Notably, the CPT1A activation was observed not only in murine models but also in butyrate-treated HCT116 cells and in patients showing resistance to anti-PD-1 therapy. CPT1A facilitates the transport of fatty acids into mitochondria, inside which starts to use the β-oxidation pathway for ATP generation [26]. As a key rate-limiting enzyme in FAO, CPT1A adjusts the fatty acid metabolism rate to meet cellular energy demands [27]. Previous studies have established the relationship between CPT1A-mediated FAO activation and cancer cell energy adaptation, facilitating tumor survival under therapeutic stress [28, 29]. In consistency with these, we observed the increase in CPT1 enzyme expression induced by butyrate treatment to HCT116 cells, which was correlated with a rise in OCR compared to controls. Remarkably, CPT1A knockdown produced the opposite effect, with a notable decrease in cellular respiration. These findings support the view that CPT1A-mediated FAO functions as a metabolic adaptation mechanism. It produces more ATP per molecule than glucose metabolism, helping tumor cells survive under stressful conditions and resist pressures from chemotherapy and targeted therapies [29, 30]. The critical role of butyrate in regulating FAO may explain the resistance of HCT116 cells to α-PD-1 during treatment at least to a certain extent.

In addition, FAO regulates immune activity within the TME through various mechanisms. For example, upregulated FAO can deplete essential nutrients like glucose and amino acids in the TME, limiting the metabolic resources available to effector T cells [31, 32]. Additionally, FAO-generated metabolites, such as lipid peroxides, arachidonic acid derivatives, and other oxidative lipids, can directly suppress T cell activity or induce the secretion of immunosuppressive cytokines like IL-10 and TGF-β, fostering an immunosuppressive environment [16, 33–35]. In the present study, our findings indicate that butyrate-induced FAO upregulation in combination with α-PD-1 similarly contributes to drug resistance in CRC via immune cell suppression. In co-culture assays with CD8+ T cells, the addition of butyrate reduced the cytotoxic effect of α-PD-1 on CRC cells. In contrast, CPT1A knockdown reversed this effect, equalizing the cytotoxicity levels between the combination therapy and α-PD-1 monotherapy. These findings highlight that CPT1A-mediated FAO inhibition could potentially reverse butyrate-induced resistance to ICIs and restore cytotoxic T cell function within the TME. Notably, in vivo outcomes demonstrated that CPT1A knockdown even enhanced the antitumor efficacy of combination therapy beyond that of immune monotherapy alone, outperforming those in vitro. This effect may be due to the complexity of in vivo regulatory pathways and environmental factors remains further study.

Our study has several limitations that should be acknowledged. We recognize that the impact of varying dosages of butyrate on tumor metabolism and therapeutic responses was not comprehensively explored in this study. Although we selected a dosage based on preliminary experiments to achieve optimal results aligned with our objectives, a systematic investigation into dose-dependent effects is essential for understanding butyrate's broader role in tumor progression and therapy resistance in future studies. Furthermore, since our study primarily focused on CPT1A's role in butyrate-mediated resistance, potential side effects of CPT1A inhibition were not directly investigated. While this was beyond the scope of the current study, understanding the adverse outcome and safety profile of targeting CPT1A is critical for its clinical application. Also, while our data showed promising correlations between its expression and therapeutic resistance in patient samples, the sample size was relatively small. In further studies, larger clinical studies incorporating baseline data would be take into consideration to enhance the applicability of our findings, allowing for a more comprehensive analysis of the relationship between CPT1A expression and resistance to anti-PD-1 therapy.

Our study demonstrated that butyrate induces resistance to anti-PD-1 therapy in CRC by promoting CPT1A-mediated FAO and CPT1A knockdown in murine models and a CRC cell line reversed this resistance, enhancing the antitumor efficacy of combined butyrate/anti-PD-1 therapy and restoring CD8 + T cell infiltration. These findings highlighted the potential of targeting CPT1A-mediated FAO as a strategy to improve response to immunotherapy in CRC.

Acknowledgements None.

Author contributions RZ and YZ designed experiments. SJG and YT carried out experiments, analyzed experimental results. RZ wrote the manuscript. YZ revised the manuscript. All authors approved the final manuscript.

Funding This research did not receive any specific grant from funding agencies in the public, commercial, or not-for-profit sectors.

Data availability The data that support the findings of this study are available from the corresponding author upon reasonable request.

Declarations

Ethics approval and consent to participate All animal experiments were conducted in accordance with the guidelines for the Care and Use of Laboratory Animals as adopted by the National Institutes of Health and were approved by the Institutional Animal Care and Use Committee of Beijing Changping Traditional Chinese Medicine Hospital. For ethics of studies related to humans, all patient samples were collected under informed consent and in accordance with the ethical standards set forth by the Declaration of Helsinki. Ethical approval for this study was obtained from the Institutional Review Board of Beijing Changping Traditional Chinese Medicine Hospital.

Competing interests The authors declare no competing interests.

References

1. Biller LH, Schrag D. Diagnosis and treatment of metastatic colorectal cancer: a review. JAMA. 2021;325(7):669–85.
2. Kumar A, Gautam V, Sandhu A, Rawat K, Sharma A, Saha L. Current and emerging therapeutic approaches for colorectal cancer: a comprehensive review. World J Gastrointest Surg. 2023;15(4):495.
3. Golshani G, Zhang Y. Advances in immunotherapy for colorectal cancer: a review. Ther Adv Gastroenterol. 2020. https://doi.org/10.1177/1756284820917527.
4. Makaremi S, Asadzadeh Z, Hemmat N, Baghbanzadeh A, Sgambato A, Ghorbaninezhad F, et al. Immune checkpoint inhibitors in colorectal cancer: challenges and future prospects. Biomedicines. 2021;9(9):1075.
5. Chen X, Chen L-J, Peng X-F, Deng L, Wang Y, Li J-J, et al. Anti-PD-1/PD-L1 therapy for colorectal cancer: clinical implications and future considerations. Transl Oncol. 2024;40:101851.
6. Wang Z, Wu X. Study and analysis of antitumor resistance mechanism of PD1/PD-L1 immune checkpoint blocker. Cancer Med. 2020;9(21):8086–121.
7. Wong CC, Yu J. Gut microbiota in colorectal cancer development and therapy. Nat Rev Clin Oncol. 2023;20(7):429–52.
8. Qu R, Zhang Y, Ma Y, Zhou X, Sun L, Jiang C, et al. Role of the gut microbiota and its metabolites in tumorigenesis or development of colorectal cancer. Adv Sci. 2023;10(23):2205563.
9. Han A, Bennett N, Ahmed B, Whelan J, Donohoe DR. Butyrate decreases its own oxidation in colorectal cancer cells through inhibition of histone deacetylases. Oncotarget. 2018;9(43):27280.
10. Li Q, Ding C, Meng T, Lu W, Liu W, Hao H, et al. Butyrate suppresses motility of colorectal cancer cells via deactivating Akt/ERK signaling in histone deacetylase dependent manner. J Pharmacol Sci. 2017;135(4):148–55.
11. Chen J, Vitetta L. Inflammation-modulating effect of butyrate in the prevention of colon cancer by dietary fiber. Clin Colorectal Cancer. 2018;17(3):e541–4.
12. Hao F, Tian M, Zhang X, Jin X, Jiang Y, Sun X, et al. Butyrate enhances CPT1A activity to promote fatty acid oxidation and iTreg differentiation. Proc Natl Acad Sci. 2021;118(22):e2014681118.
13. Kant S, Kesarwani P, Prabhu A, Graham SF, Buelow KL, Nakano I, et al. Enhanced fatty acid oxidation provides glioblastoma cells metabolic plasticity to accommodate to its dynamic nutrient microenvironment. Cell Death Dis. 2020;11(4):253.
14. Elia I, Haigis MC. Metabolites and the tumour microenvironment: from cellular mechanisms to systemic metabolism. Nat Metab. 2021;3(1):21–32.
15. Hoy AJ, Nagarajan SR, Butler LM. Tumour fatty acid metabolism in the context of therapy resistance and obesity. Nat Rev Cancer. 2021;21(12):753–66.
16. Reina-Campos M, Scharping NE, Goldrath AW. CD8+ T cell metabolism in infection and cancer. Nat Rev Immunol. 2021;21(11):718–38.
17. Chen Y, Liu C, Zhu S, Liang X, Zhang Q, Luo X, et al. PD-1/PD-L1 immune checkpoint blockade-based combinational treatment: immunotherapeutic amplification strategies against colorectal cancer. Int Immunopharmacol. 2021;96:107607.
18. Manitz J, D'Angelo SP, Apolo AB, Eggleton SP, Bajars M, Bohnsack O, et al. Comparison of tumor assessments using RECIST 1.1 and irRECIST, and association with overall survival. J ImmunCancer. 2022. https://doi.org/10.1136/jitc-2021-003302.

19. Taniura T, Iida Y, Kotani H, Ishitobi K, Tajima Y, Harada M. Immunogenic chemotherapy in two mouse colon cancer models. Cancer Sci. 2020;111(10):3527–39.
20. MacArthur Clark JA, Sun D. Guidelines for the ethical review of laboratory animal welfare People's Republic of China National Standard GB/T 35892–2018 (Issued 6 February 2018 effective from 1 September 2018). Anim Models Exp Med. 2020;3(1):103–13.
21. Adebayo AS, Agbaje K, Adesina SK, Olajubutu O. Colorectal cancer: disease process, current treatment options, and future perspectives. Pharmaceutics. 2023;15(11):2620.
22. Shu Y, Zheng S. The current status and prospect of immunotherapy in colorectal cancer. Clin Transl Oncol. 2024;26(1):39–51.
23. Guan X, Li W, Meng H. A double-edged sword: role of butyrate in the oral cavity and the gut. Mol Oral Microbiol. 2021;36(2):121–31.
24. Okumura S, Konishi Y, Narukawa M, Sugiura Y, Yoshimoto S, Arai Y, et al. Gut bacteria identified in colorectal cancer patients promote tumourigenesis via butyrate secretion. Nat Commun. 2021;12(1):5674.
25. Kang X, Liu C, Ding Y, Ni Y, Ji F, Lau HCH, et al. Roseburia intestinalis generated butyrate boosts anti-PD-1 efficacy in colorectal cancer by activating cytotoxic CD8+ T cells. Gut. 2023;72(11):2112–22.
26. Schlaepfer IR, Joshi M. CPT1A-mediated fat oxidation mechanisms and therapeutic potential. Endocrinology. 2020. https://doi.org/10.1210/endocr/bqz046.
27. Tang M, Dong X, Xiao L, Tan Z, Luo X, Yang L, et al. CPT1A-mediated fatty acid oxidation promotes cell proliferation via nucleoside metabolism in nasopharyngeal carcinoma. Cell Death Dis. 2022;13(4):331.
28. Han S, Wei R, Zhang X, Jiang N, Fan M, Huang JH, et al. CPT1A/2-mediated FAO enhancement—a metabolic target in radioresistant breast cancer. Front Oncol. 2019;9:1201.
29. De Oliveira MP, Liesa M. The role of mitochondrial fat oxidation in cancer cell proliferation and survival. Cells. 2020;9(12):2600.
30. Xiong X, Wen Y-A, Fairchild R, Zaytseva YY, Weiss HL, Evers BM, et al. Upregulation of CPT1A is essential for the tumor-promoting effect of adipocytes in colon cancer. Cell Death Dis. 2020;11(9):736.
31. Zhao S, Peralta RM, Avina-Ochoa N, Delgoffe GM, Kaech SM. Metabolic regulation of T cells in the tumor microenvironment by nutrient availability and diet. Semin Immunol. 2021. https://doi.org/10.1016/j.smim.2021.101485.
32. Tang Y, Chen Z, Zuo Q, Kang Y. Regulation of CD8+ T cells by lipid metabolism in cancer progression. Cell Mole Immunol. 2024. https://doi.org/10.1038/s41423-024-01224-z.
33. Xu S, Chaudhary O, Rodríguez-Morales P, Sun X, Chen D, Zappasodi R, et al. Uptake of oxidized lipids by the scavenger receptor CD36 promotes lipid peroxidation and dysfunction in CD8+ T cells in tumors. Immunity. 2021;54(7):1561-77.e7.
34. Zheng M, Zhang W, Chen X, Guo H, Wu H, Xu Y, et al. The impact of lipids on the cancer–immunity cycle and strategies for modulating lipid metabolism to improve cancer immunotherapy. Acta Pharm Sin B. 2023;13(4):1488–97.
35. Shi X, Yang J, Deng S, Xu H, Wu D, Zeng Q, et al. TGF-β signaling in the tumor metabolic microenvironment and targeted therapies. J Hematol Oncol. 2022;15(1):135.